



CHAPTER IV

RESULTS AND DISCUSSION

4.1 Catalyst Characterization

4.1.1 XRD Patterns

The XRD patterns of pure FeO_x , and MnO_x supports are shown in Figure 4.1 (patterns a, and e). The distinct peaks illustrated that the synthesized FeO_x support has $\alpha\text{-Fe}_2\text{O}_3$ formed in hematite phase (JCPDS 33-0664) at 2θ of 24.15° , 33.15° , 35.65° , 40.85° , 49.50° , 54.10° , 57.60° , 62.45° , 64.05° , 71.95° , and 75.5° , respectively. Typical XRD patterns of MnO_2 (JCPDS 44-0141) were observed over the synthesized MnO_x at 2θ of 37.30° and 42.50° .

The XRD patterns in Figure 4.1 shows the differences between XRD patterns of pure FeO_x , MnO_x (patterns a and e), and supported Au catalysts. The deposition of Au on the supports (FeO_x , MnO_x , and $\text{FeO}_x\text{-MnO}_x$) resulted in a decrease in intensity of FeO_x and MnO_x . The spectrum of the Au/FeO_x sample (pattern d) shows only the XRD peaks of a Fe_2O_3 hematite phase, which is the same as in the case of FeO_x support (pattern e). However, the intensities of the peaks are reduced. For the MnO_x support (pattern a), the peaks of MnO_2 are observed at $2\theta = 37.30^\circ$ and 42.50° . In the Au/MnO_x sample (pattern b), the peaks of gold could be observed. The XRD patterns of $\text{Au/FeO}_x\text{-MnO}_x$ (pattern c), the characteristic peaks of Fe_2O_3 or MnO_2 could not be detected. In addition, the metallic Au species attributed to Au (111), Au (200), Au (220), and Au (311) peaks are clearly observed at 2θ of 38.2° , 44.4° , 64.6° , and 77.7° , respectively, for Au/MnO_x and $\text{Au/FeO}_x\text{-MnO}_x$. No peaks of metallic Au are observed implying that Au is well dispersed on the catalyst surface or that gold particles is small than 5 nm. According to Luengnaremitchai *et al.* (2005), the limitations of XRD for gold crystallites correspond to a particle size smaller than 5 nm could not be detected by this instrument.

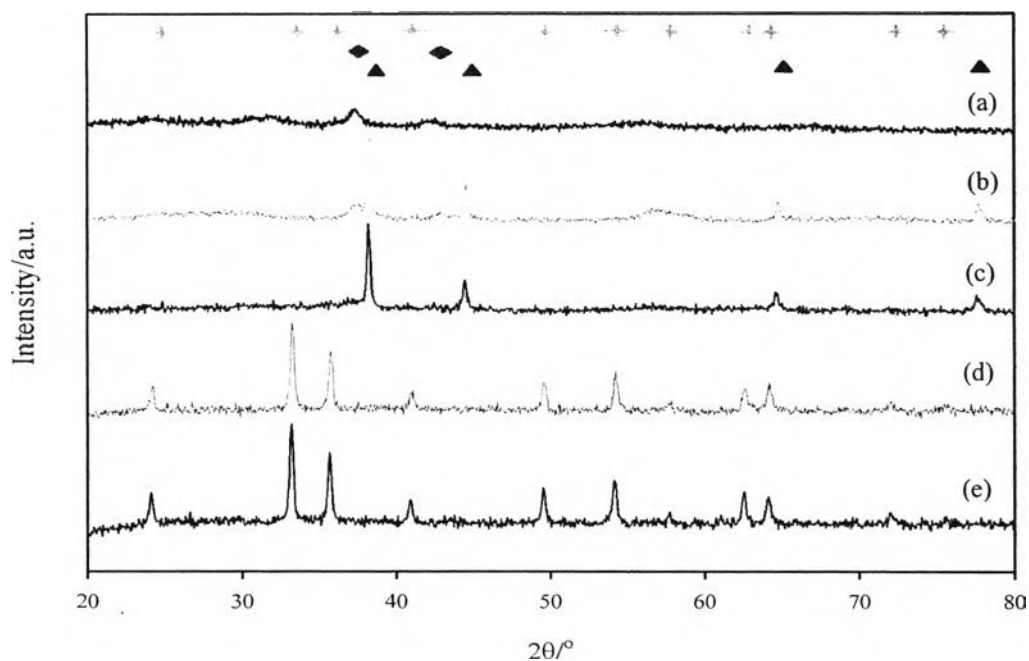


Figure 4.1 XRD patterns of catalysts calcined at 400°C: (a) MnO_x without Au loading; (b) MnO_x ; (c) $\text{FeO}_x\text{-MnO}_x$ (1:1 molar ratio); (d) FeO_x with Au loading at 1/30 atomic ratio; and (e) FeO_x without Au loading: (+) Fe_2O_3 ; (◆) MnO_2 ; (▲) Au.

Figure 4.2 represents the XRD pattern of the $\text{Au/FeO}_x\text{-MnO}_x$ catalysts with different Au loading. At low gold loading, the diffraction peaks of metallic gold were observed. Increasing the amount of gold the intensities of metallic gold peaks are observed.

The crystalline phase of $\text{Au/FeO}_x\text{-MnO}_x$ calcined at 400°C were determined from XRD measurements. X-ray patterns of catalyst with different $\text{FeO}_x\text{-MnO}_x$ molar ratio are illustrated in Figure 4.3. It revealed that the samples with molar ratios of $\text{FeO}_x\text{-MnO}_x$ of 5:1 and 10:1 consisted of $\alpha\text{-Fe}_2\text{O}_3$ phase. On the other hand, the characteristic peaks of MnO_2 could not be detected in the all samples. For the sample with 1:1, 1:5, and 1:10 molar ratios of $\text{FeO}_x\text{-MnO}_x$, additional peaks corresponding to Au^0 metal (110), (200), (220), and (311) are clearly seen.

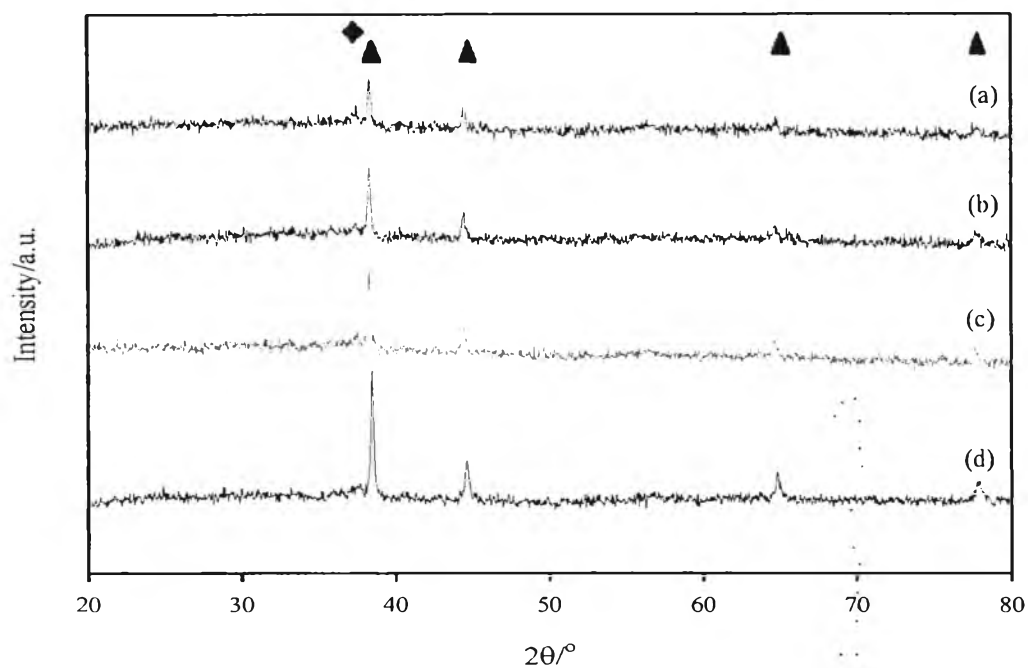


Figure 4.2 XRD patterns of catalysts calcined at 400°C, 1:1 molar ratio of mix-oxide support ($\text{FeO}_x\text{-MnO}_x$) with different Au/ $\text{FeO}_x\text{-MnO}_x$ atomic ratios: (a) 1/120; (b) 1/60; (c) 1/45; (d) 1/30: (○) Fe_2O_3 ; (◆) MnO_2 ; (▲) Au.

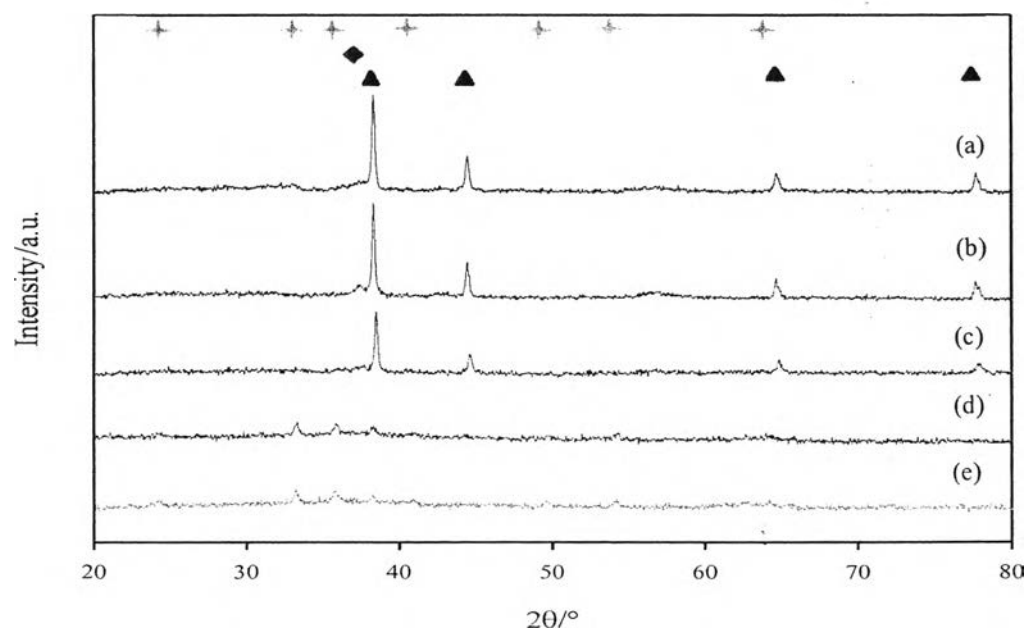


Figure 4.3 XRD patterns of catalysts calcined at 400°C, 1/30 atomic ratio of Au loading with different support molar ratios ($\text{FeO}_x\text{-MnO}_x$): (a) 1:10; (b) 1:5; (c) 1:1; (d) 5:1; (e) 10:1: (○) Fe_2O_3 ; (◆) MnO_2 ; (▲) Au.

Figure 4.4 compares the spectra of Au/FeO_x-MnO_x catalyst after calcination at three different temperatures (300°C, 400°C, 500°C). In all spectra typical reflection of Au (the metallic gold); however, the reflection of Fe₂O₃ and MnO₂ can be observed for samples calcined at 500°C.

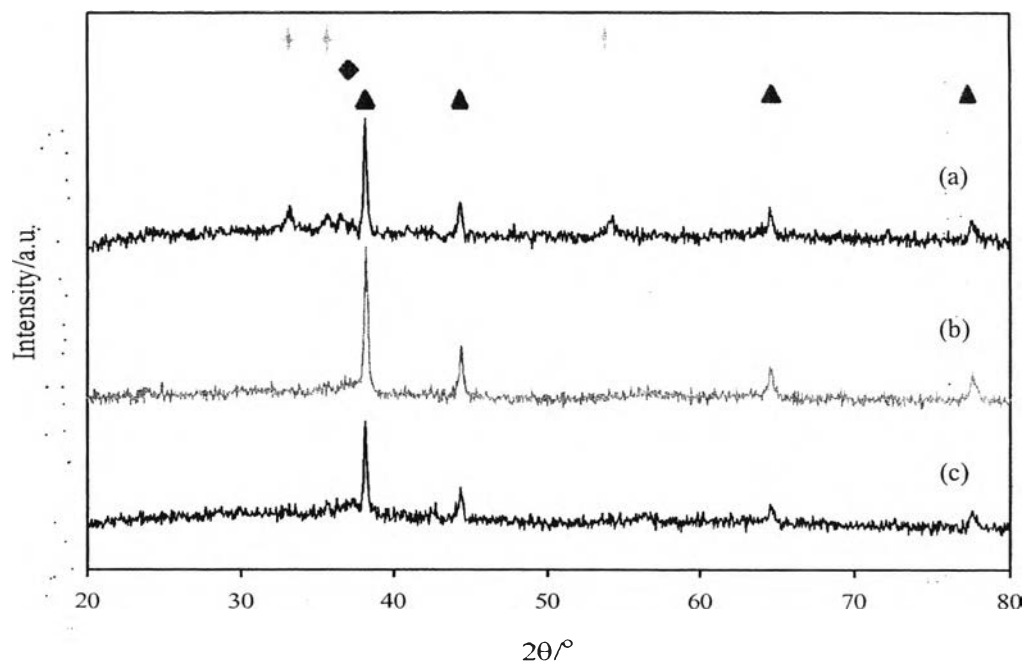


Figure 4.4 XRD patterns of catalysts calcined at different temperatures: (a) 500°C; (b) 400°C; (c) 300°C with 1/30 atomic ratio of Au loading, and 1:1 molar ratio of mix-oxide support (FeO_x-MnO_x): (+) Fe₂O₃; (◆) MnO₂; (▲) Au.

Figure 4.5 shows the XRD patterns of the catalysts as prepared and the differently pretreated Au/FeO_x-MnO_x as well as the spent catalyst. It can be seen that catalyst pretreated with O₂ showed as same Au peak intensity as fresh catalyst even if this catalyst was used. Catalyst pretreated with O₂ also exhibited peak intensity of Au lower than non-pretreatment, and He pretreatment, respectively after reaction occurred. It may be implied that the catalyst pretreated by O₂ can be inhibited Au agglomeration on the catalyst surface.

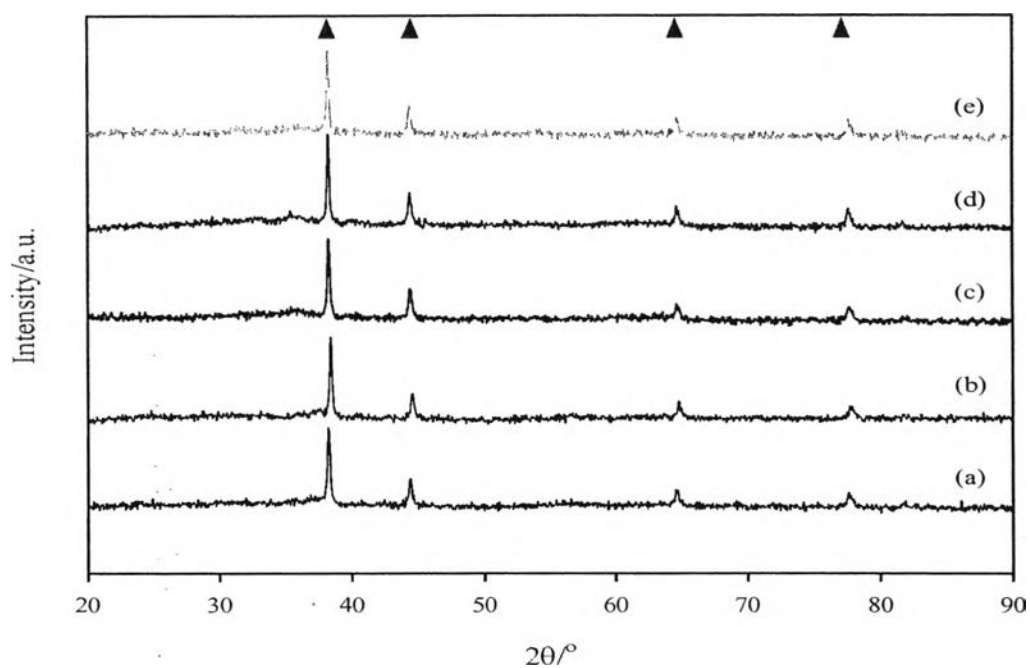


Figure 4.5 XRD patterns of fresh catalyst (a); spent catalysts with different pretreatment condition: (b) O_2 pretreatment; (c) non-pretreatment; (d) He pretreatment; and spent catalyst after stability test in PROX reactor (e) calcined at 400°C , 1/30 atomic ratio of Au loading, 1/1 molar ratio of support ($\text{FeO}_x\text{-MnO}_x$): (\blacktriangle) Au.

4.1.2 UV Measurement

The DR/UV-vis spectroscopy is used to analyze gold species. The observation of gold nanoparticles (plasmon), gold clusters (Au_n , $1 < n < 10$), and Au^{3+} species displays at 550, 280-380, and less than 250 nm (Souza *et al.*, 2008), respectively. Figures 4.6-4.9 show the diffuse reflectance UV-vis spectra of samples which occur around 350 nm and related to Au clusters (Souza *et al.*, 2008). In addition, the supported Au catalysts exhibit a band at 550 nm which could be taken as an indication of the existence of metallic Au particles. Therefore it is assumed that both metallic and Au charged cluster are present on these samples.

Figure 4.7 represents the spectra of catalysts with different molar ratio of $\text{FeO}_x\text{-MnO}_x$ exhibited a broad band with maximum at 360 nm, which corresponds to oxidation states of Au clusters (Deng *et al.*, 2007). It was found that the Au catalyst with support molar ratio (Fe/Mn) of 1/1 had the weakest absorbance of Au clusters when compared with others.

Figure 4.8 compared the calcination temperature of the prepared catalysts, it can be observed that the high calcinaion temperature affected to a decrease in intensity of Au clusters at 360 nm.

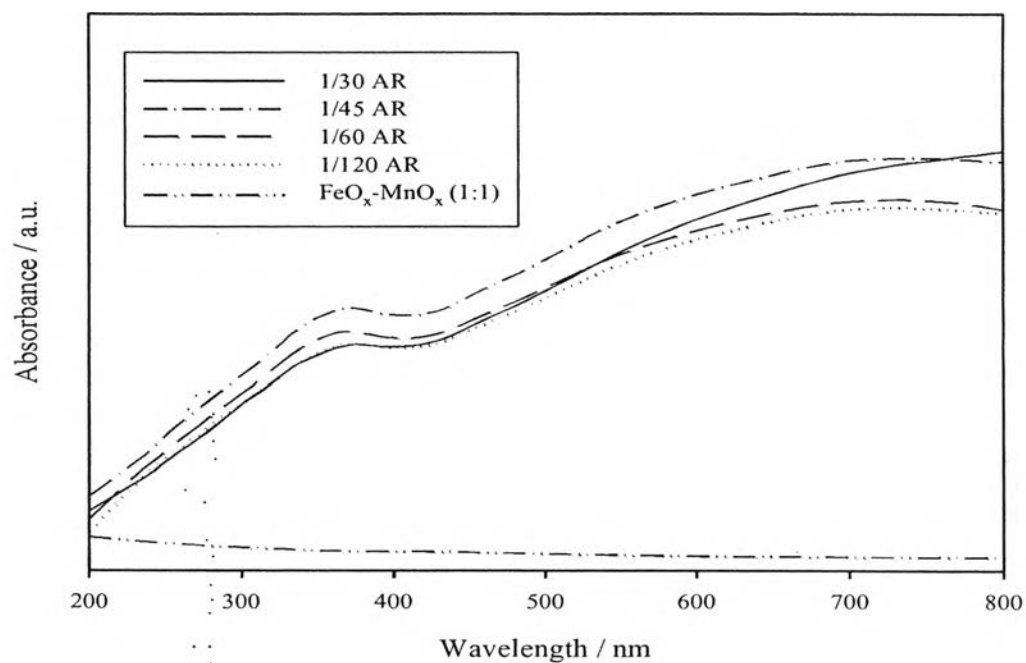


Figure 4.6 UV-vis spectra of catalysts calcined at 400°C, support molar ratio (Fe/Mn) of 1/1 with different Au/FeO_x-MnO_x atomic ratios (AR).

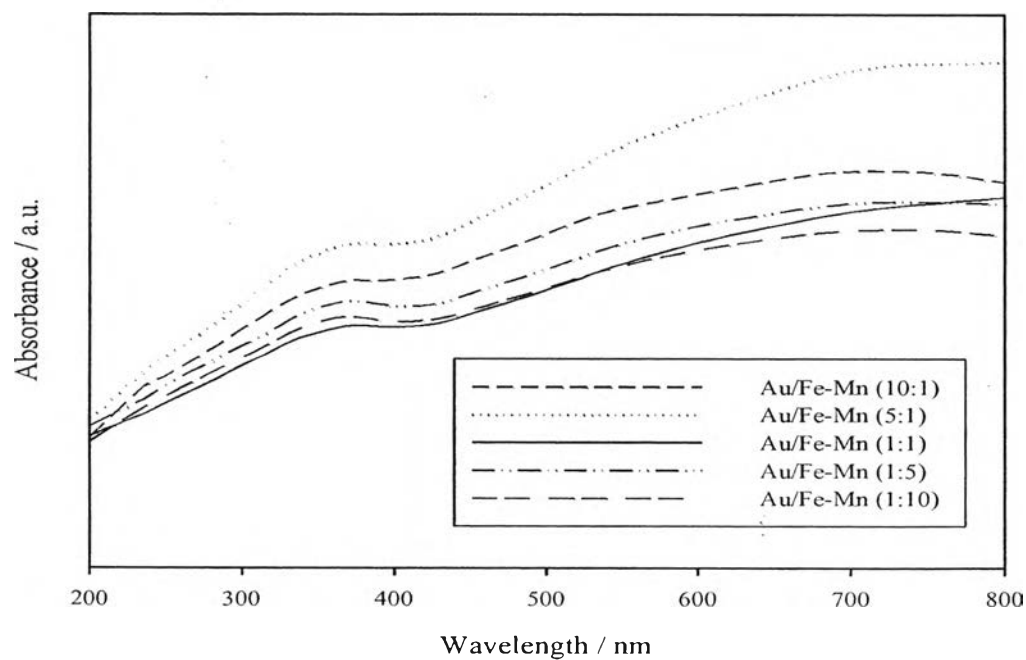


Figure 4.7 UV-vis spectra of catalysts calcined at 400°C, Au/FeO_x-MnO_x atomic ratio of 1/30 with different support molar ratios (Fe/Mn).

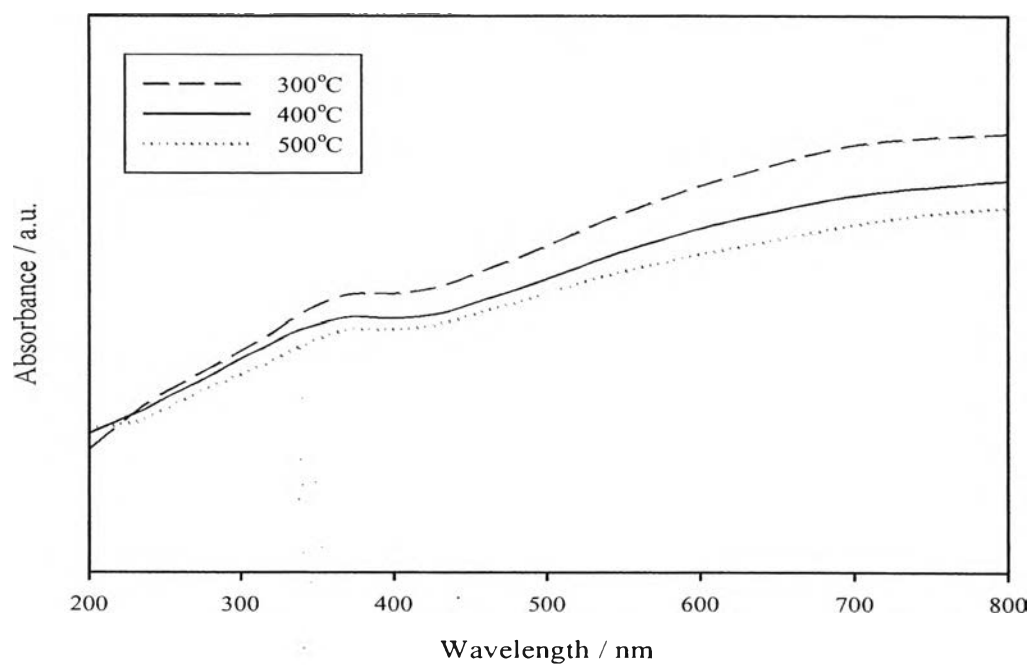


Figure 4.8 UV-vis spectra of Au/FeO_x-MnO_x catalyst at a Au/FeO_x-MnO_x atomic ratio of 1/30, support molar ratio (Fe/Mn) of 1/1 with different calcination temperatures.

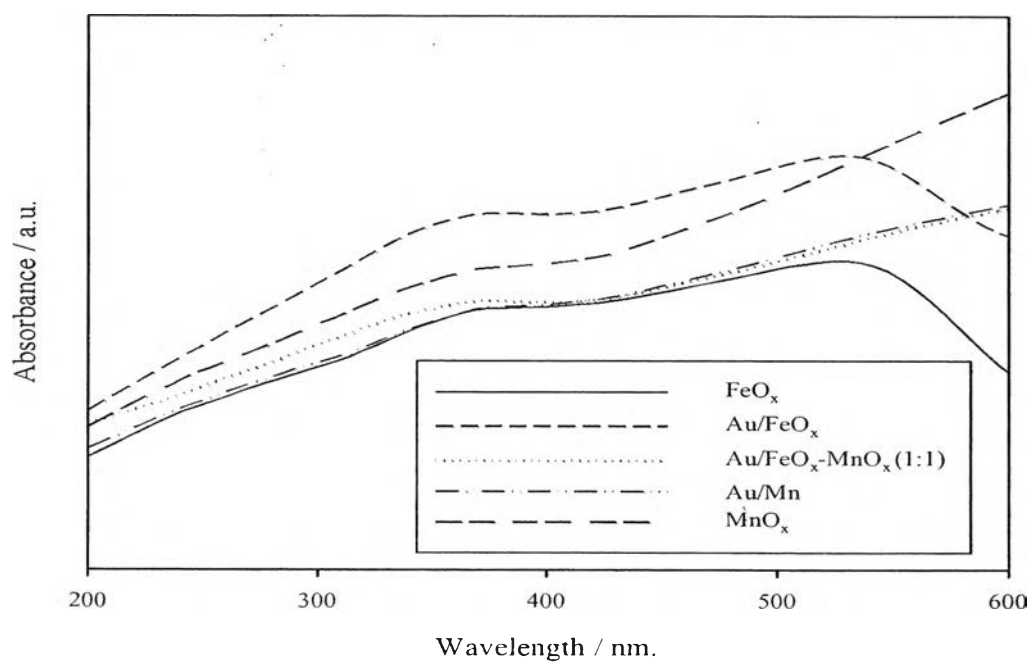


Figure 4.9 UV-vis spectra of FeO_x, Au/FeO_x, Au/FeO_x-MnO_x, Au/MnO_x, and MnO_x catalysts.

4.1.3 TPR Measurement

The temperature-programmed reduction (TPR) is a convenient technique applied for studying the reduction behavior of the unpromoted and supported Au catalyst. Figure 4.10 shows the TPR profiles for FeO_x , $\text{FeO}_x\text{-MnO}_x$ (1:1), Au/FeO_x , Au/MnO_x , and for $\text{Au/FeO}_x\text{-MnO}_x$ with different Au content of 1/120, 1/60, 1/45, and 1/30 atomic ratio, respectively. The bulk iron oxide showed two distinct reduction peaks with values of T_{max} of 447 and 689°C. The first reduction peak at 447°C attributed to the reduction of Fe_2O_3 (hematite) to Fe_3O_4 (magnetite) was observed (Venugopal *et al.*, 2004). The high temperature reduction peak at 689°C is attributed to the reduction of Fe_3O_4 (magnetite) to FeO species (Venugopal *et al.*, 2004).

For $\text{Au/Fe}_2\text{O}_3$ catalyst at 1/30 atomic ratio, three reduction peaks at 149, 350, and 687°C were found, respectively. The reduction peaks centered at 149°C is attributed to the reduction of Au_xO_y species in $\text{Au/Fe}_2\text{O}_3$ (Venugopal *et al.*, 2004). It is pointed out that $\text{Au/Fe}_2\text{O}_3$ catalyst had some interaction between Au and support. According to shifted reduction peak in bulk Fe_2O_3 from 447 to 350°C indicating that the positive influence on Au facilitates reduction of Fe_2O_3 at the lower temperature. Wang *et al.*, 2002 concentrated to study the catalytic behavior of $\text{Au/Fe}_2\text{O}_3$. Interestingly, the high temperature reduction peak around 689°C in both bulk Fe_2O_3 and $\text{Au/Fe}_2\text{O}_3$ (1/30 atomic ratio) has quite the same value which can refer to the reduction of Fe_3O_4 in both catalyst. On the other hand, the usually XRD analysis result exhibited only peaks of metallic Au but did not expose the any Au-oxidic species (Venugopal *et al.*, 2004). The possibility absence Au_xO_y species from XRD analysis are low concentration, amorphous intensity, and very small crystallite size (nanosized), either (Venugopal *et al.*, 2004).

For Au/MnO_2 (1/30 atomic ratio), there are two overlapped peaks with the maximum value of 376 and 503°C as shown in Figure 4.10. Evidently, these two peaks can be assigned to the two steps reduction of MnO_2 (Ramesh *et al.*, 2008). The first reduction step at 376°C corresponding to the reduction of MnO_2 to Mn_3O_4 and the second reduction step at 503°C attributing to the reduction of Mn_3O_4 to MnO_2 .

The TPR profiles of $\text{FeO}_x\text{-MnO}_x$ (curve d) prepared by coprecipitation depicted that there were three interval reduction processes; (1) 300-400°C; (2) 500-

600°C; and 600-800°C, as displayed in Figure 4.10. The first interval represented to the reduction of Fe_2O_3 (hematite) to Fe_3O_4 (magnetite), the second interval corresponding to transformation of Fe_3O_4 (magnetite) to FeO and MnO phase, and the last interval took place at the maximum high temperature due to the reduction of FeO to Fe and MnO (Oliveira *et al.*, 2004). After a small amount of gold was added on comprised support (1/120 atomic ratio), the reduction temperature peak shifted to higher temperature when compare with reducible mixed oxide support. This reduction behavior suggested that this catalyst had been partially reduced by the incomplete decomposition of precursor before H_2 TPR measurement (Zhang *et al.*, 2009). Simultaneously, the increase of Au content had remarkably higher reducibility than low Au content. Talking into account the changes of the reducibility peak at lower temperature of the increase Au content, it was supposed that the rate of reduction of Fe-Mn oxide solids was affected by Au content. Furthermore, the catalyst could be easily reduced at lower temperature corresponding to higher responsibility to adsorb H_2 was mostly due to the smaller particle sizes, better particle dispersion, and higher surface area. The definition of this phenomenon was described by Solsona *et al.*, 2006. The presence of Au on any oxide support could improve redox properties, possibly due to the surface defect on the support. Especially, these effects may be related to the formation of the new sites at interface between the Au nanoparticles and the oxide surface. From TPR result in Figure 4.10, it was notably discovered that the increasing of Au on $\text{FeO}_x\text{-MnO}_x$ oxide lead to decrease the metal support interaction. It can refer to the moving a large cluster size facilitates to overcome this interaction, implying that the large metal clusters for higher amount of Au content are more easily reduce (Jacobs *et al.*, 2005).

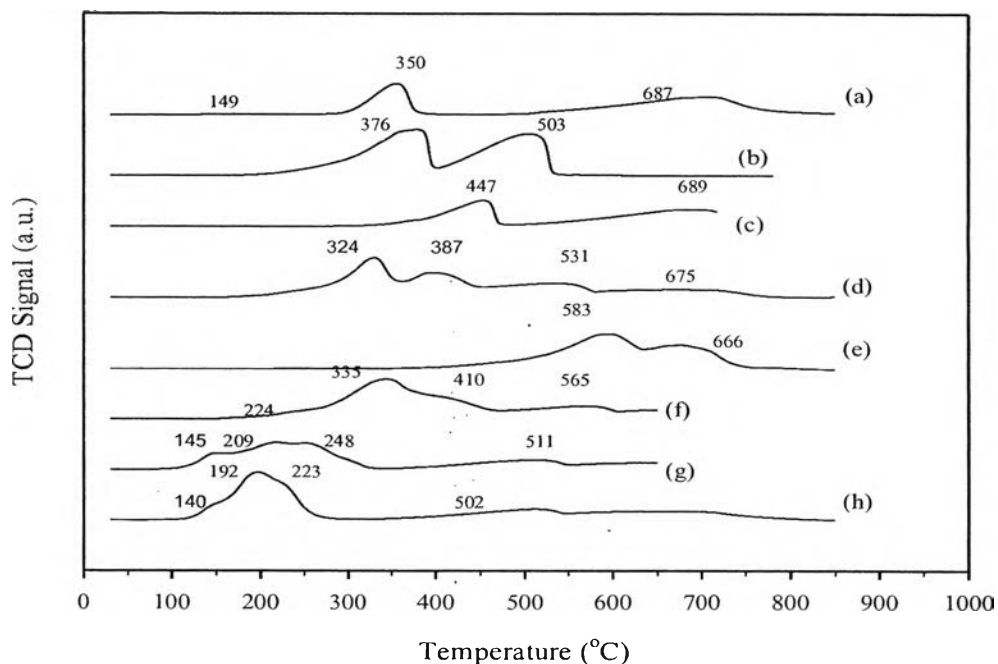


Figure 4.10 TPR profiles of unpromoted and promoted Au catalysts over different supports: (a) 1/30 atomic ratio of Au/FeO_x; (b) 1/30 atomic ratio of Au/MnO_x; (c) FeO_x; (d) 1/1 molar ratio of FeO_x-MnO_x; (e) 1/120 atomic ratio of Au/FeO_x-MnO_x; (f) 1/60 atomic ratio of Au/FeO_x-MnO_x; (g) 1/45 atomic ratio of Au/FeO_x-MnO_x; (h) 1/30 atomic ratio of Au/FeO_x-MnO_x.

Figure 4.11 shows the TPR profiles of Au/FeO_x-MnO_x mixed oxides FeO_x-MnO_x with different molar ratios of FeO_x/MnO_x. The Fe/Mn molar ratio were varied from 10/1 to 5/1, 1/1, 1/5, and 1/10 at a Au/FeO_x-MnO_x atomic ratio of 1/30, as shown on Figure 4.12. It is clearly seen that the reducibility on binary oxides shows an order of 1/1 > 10/1 ≅ 5/1 >> 1/5 > 1/10 in a molar ratio (Fe/Mn) at lower temperature. It revealed that Au/FeO_x-MnO_x (1:1) was more easily reduced at lower temperature compared to other catalysts.

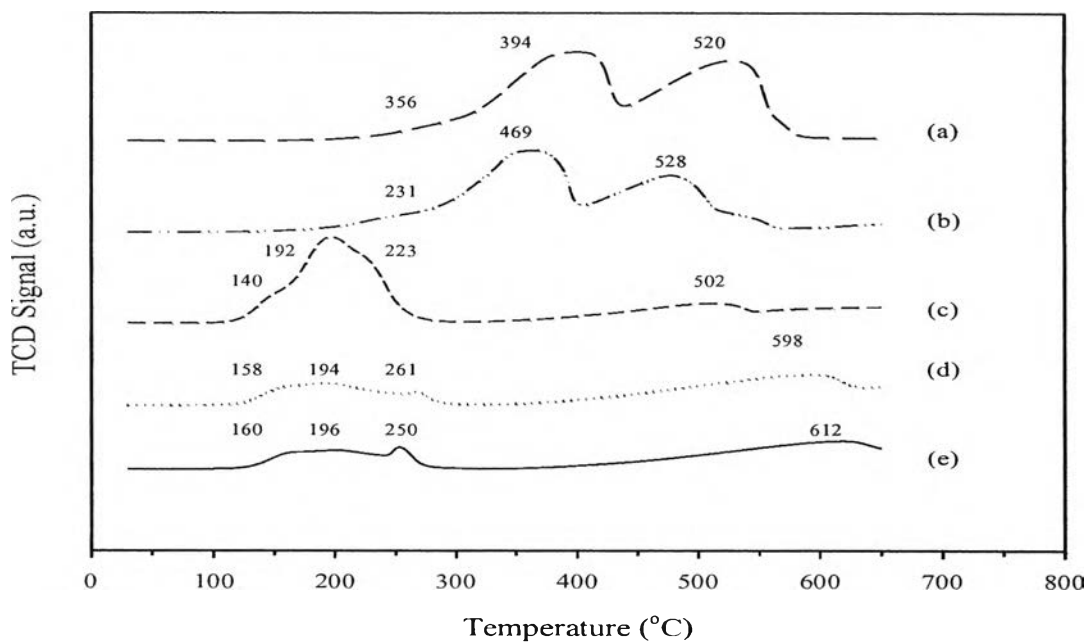


Figure 4.11 TPR profiles of catalysts calcined at 400°C, Au/FeO_x-MnO_x atomic ratio of 1/30 with different support molar ratios (FeO_x-MnO_x): (a) 1:10; (b) 1:5; (c) 1:1; (d) 5:1; (e) 10:1.

Figure 4.12 shows the H₂-TPR results of Au/FeO_x-MnO_x atomic ratio of 1/30 and Fe/Mn molar ratio of 1/1 samples calcined at 300°C and 400°C. Higher calcination temperature (e.g., 400°C) pivotal significantly changes the H₂-TPR profile of Au/FeO_x-MnO_x catalyst. The region of reduction peaks amplify remarkably after calcined at 400°C, and the onset reduction temperature of Au catalyst shifts to lower temperature. As gold promoter can act as a reductor, this increase in the pretreatment temperature can modify the weakness of the interaction bond between gold and Fe-Mn oxide (weak metal support interaction), some reduction of Au species also take place, leading to a remarkable change of onset reduction temperature in TPR profile.

The reduction peaks of gold-free and gold-containing catalysts are summarized in Table 4.1.

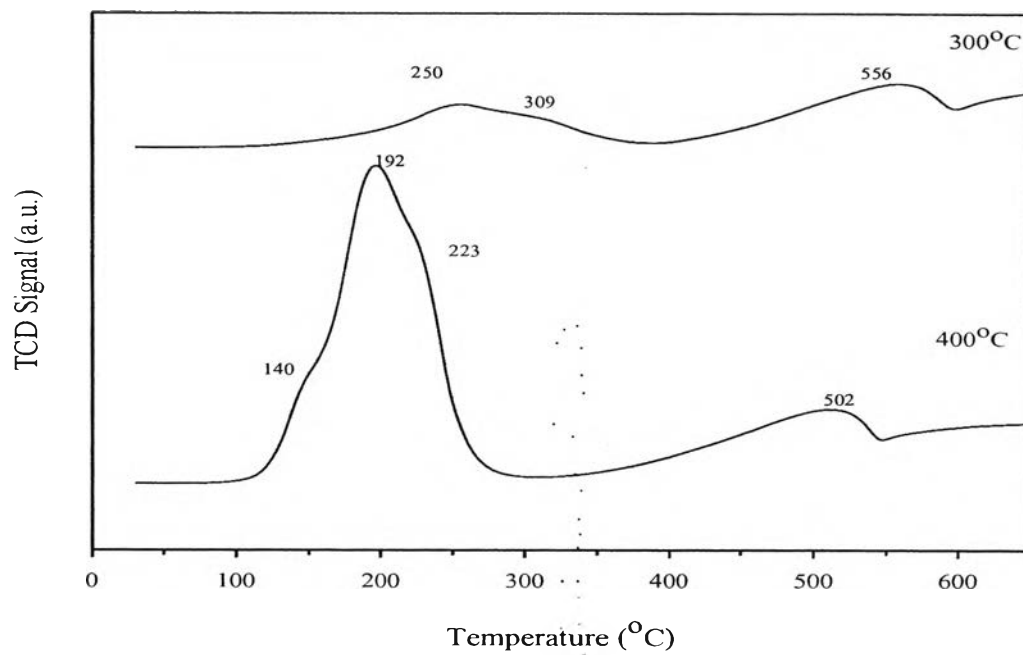


Figure 4.12 TPR profiles of Au/FeO_x-MnO_x (1:1) atomic ratio of 1/30 calcined at 300 and 400°C.

Table 4.1 Reduction peaks of gold-free and gold-containing catalysts

Type of Catalyst	Au species reduction	Fe ₂ O ₃ →Fe ₃ O ₄		Fe ₃ O ₄ →FeO	FeO→Fe ⁰	
		Peak 1	Peak 2	Peak 3	Peak 4	Peak 5
		(T, °C)	(T, °C)	(T, °C)	(T, °C)	(T, °C)
1/30 AR ^{(b),(c)} Au/FeO _x	149	350		687	-	
1:1 MR ^(c) FeO _x -MnO _x ^(c)	-	324	387	531	675	
1/120 AR ^{(b),(c)} Au/FeO _x -MnO _x	-	538	666	-	-	
1/60 AR ^{(b),(c)} Au/FeO _x -MnO _x	224	335	410	565	-	
1/45 AR ^{(b),(c)} Au/FeO _x -MnO _x	145	209	248	511	-	
1/30 AR ^{(b),(c)} Au/FeO _x -MnO _x	140	192	223	502	673	
5:1 MR ^{(a),(c)} Au/FeO _x -MnO _x	158	194	261	598	-	
10:1 MR ^{(a),(c)} Au/FeO _x -MnO _x	160	196	250	612	-	
300°C ^{(a),(b)} Au/FeO _x -MnO _x	-	250	309	556	-	

Type of Catalyst	Au species reduction	MnO ₂ →Mn ₃ O ₄		Mn ₃ O ₄ →MnO	MnO→Mn ⁰
		Peak 1	Peak 2	Peak 3	Peak 4
		(T, °C)	(T, °C)	(T, °C)	(T, °C)
1/30 AR ^{(b),(c)} Au/MnO _x	-	376	503	-	-
1:5 MR ^{(a),(c)} Au/FeO _x -MnO _x	231	356	469	528	-
1:10 MR ^{(a),(c)} Au/FeO _x -MnO _x	-	394	520	-	-

Atomic ratio (AR)

Molar ratio (MR)

^a Au/FeO_x-MnO_x atomic ratio of 1/30^b Support molar ratio (Fe/Mn) of 1/1^c Calcination temperature of 400°C

4.1.4 BET Surface Area Measurement

The BET surface areas of unpromoted and supported Au catalysts were determined from nitrogen adsorption isotherm, the corresponding results are shown in Table 4.2. The BET surface area of the $\text{FeO}_x\text{-MnO}_x$ was $168.46 \text{ m}^2/\text{g}$. After loading Au, the surface areas of all catalyst were between 169.42 and $118.97 \text{ m}^2/\text{g}$. It was seen that a little amount of Au loading has remarkably decreased the BET surface area of the prepared catalyst. Then, the increasing proportion amount of Au resulted in a significant increase the BET surface area of $\text{Au/FeO}_x\text{-MnO}_x$. From the results, it can be illustrated that the surface area of catalysts seem to be affected by various properties, including the size of the oxide crystallites and Au particles and the structure and size of the oxide pores.

Table 4.2 BET surface areas of prepared catalysts

Type of catalyst	Fe/Mn (molar ratio)	Gold (atomic ratio)	Calcination temperature (°C)	BET surface area (m^2/g)
$\text{FeO}_x\text{-MnO}_x$	1/1	-	400	168.46
$\text{Au/FeO}_x\text{-MnO}_x$	1/1	1/120	400	118.97
	1/1	1/60	400	121.91
	1/1	1/45	400	142.03
	1/1	1/30	400	169.42

4.1.5 AAS Measurement

Table 4.3 shows the actual Au loading of Au/FeO_x, Au/MnO_x, and Au/FeO_x-MnO_x catalysts obtained by AAS. AAS measurement show that the actual gold loading close to the target Au loading; however a little lower than the target value plausibly due to either Au loss in the preparation or the washing steps. The Au/FeO_x and Au/MnO_x have the percentage of Au loading of 9.48 and 9.55 %wt., respectively. Furthermore, the percentage of Au loading of 3.25, 5.53, 6.14, and 9.58 %wt were obtain for with a Au/FeO_x-MnO_x atomic ratios of 1/120, 1/45, 1/60, and 1/30, respectively. In addition, the amount of actual Au loading of catalyst calcined at 300°C and 400°C were 9.50 %wt and 9.58 %wt, respectively.

Table 4.3 Actual Au loading on the prepared catalysts

Type of catalyst	Fe/Mn (molar ratio)	Gold (atomic ratio)	Calcination temperature (°C)	Actual* Au loading (% wt)
Au/FeO _x	-	1/30	400	9.48
Au/MnO _x	-	1/30	400	9.55
Au/FeO _x -MnO _x	1/1	1/120	400	3.25
	1/1	1/60	400	5.53
	1/1	1/45	400	6.14
	1/1	1/30	400	9.58
	10/1	1/30	400	9.53
	5/1	1/30	400	9.42
	1/5	1/30	400	9.65
	1/10	1/30	400	9.67
	1/1	1/30	300	9.50

*From AAS result

4.2 Activity Measurement

The reaction was carried out in a fixed-bed reactor as described previously packed with 100 mg catalyst of 80–120 mesh in size. The feed gas consisted of 1% CO, 1% O₂, and 40% H₂ balanced in He passing through the catalyst bed at a total flow rate of 50 ml/min (SV=30,000 mlg⁻¹h⁻¹) under atmospheric pressure.

4.2.1 Effect of Au Loading

PROX of CO reaction was carried out over Au/FeO_x-MnO_x catalysts calcined at 400°C with various atomic ratios of 1/30–1/120 in the reaction temperature range of 60 to 180°C. The catalytic activity could depict that a higher Au content gave higher CO conversion at low temperatures. On the other hand, the small Au content gave the high CO conversion at high temperatures as shown in Figure 4.13. Among the prepared catalysts, both catalysts with atomic ratios of 1/30 and 1/45 Au/FeO_x-MnO_x, exhibited the highest CO conversion (100%) at 60°C, which the nearest optimum condition for PEMFC application (~80–120°C); however, both of them did not show significantly difference in term of CO conversion. Nevertheless, it had apparent difference in term of PROX selectivity. The Au/FeO_x-MnO_x with a 1/30 atomic ratio gave higher PROX selectivity than 1/45 atomic ratio in the wide operating temperature (60–120°C). Hence, the catalyst with Au loading at 1/30 atomic ratio was selected as the optimum condition for Au/FeO_x-MnO_x catalyst, which provided almost 100% CO conversion and 56% PROX selectivity (CO selectivity) at 60°C.

In this work, it was found that the highest activities were observed for the Au/FeO_x-MnO_x with a Au/FeO_x-MnO_x atomic ratio of 1/30 with the highest surface area (Table 4.2).

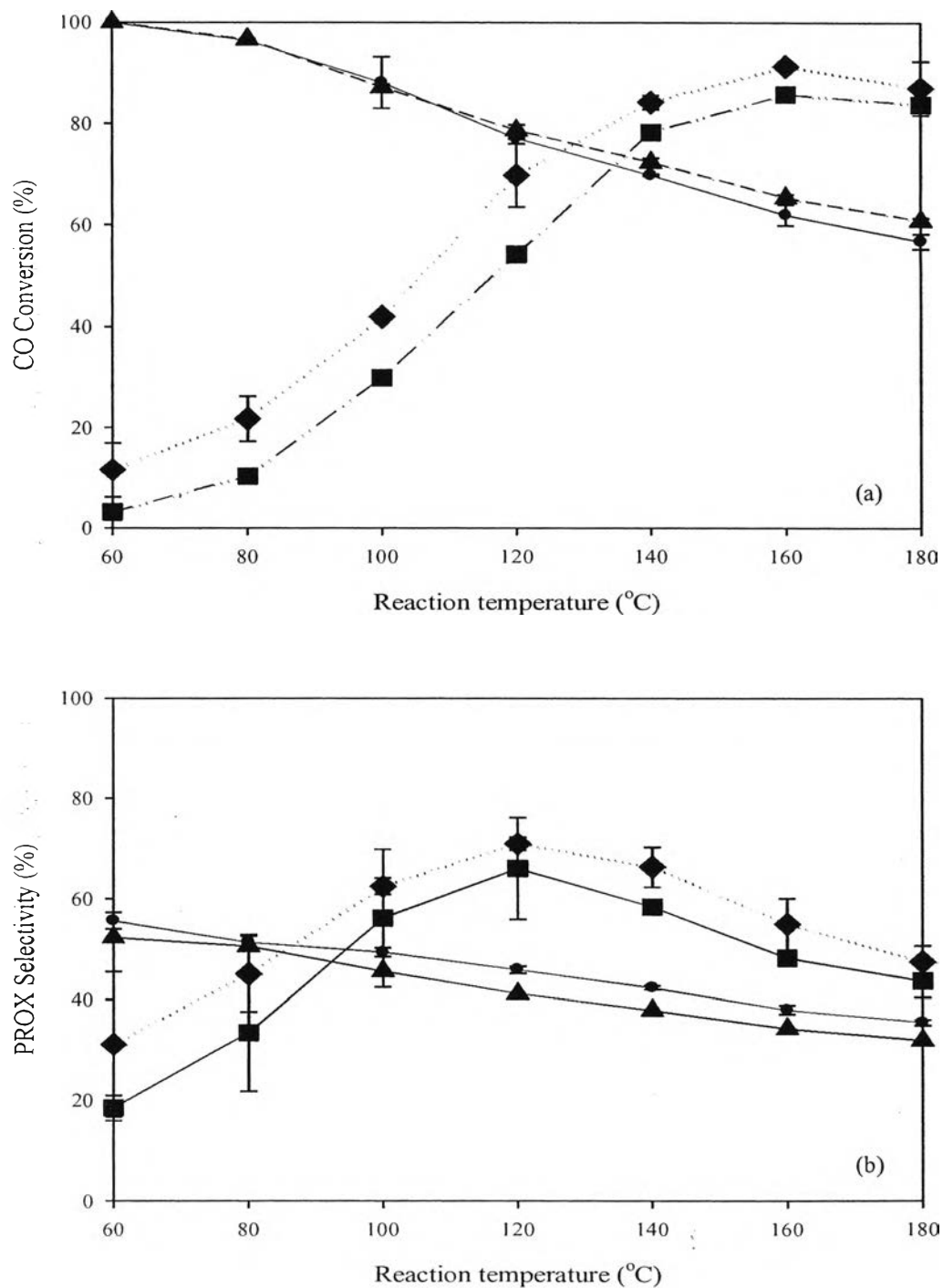


Figure 4.13 Effect of Au loading on Au/FeO_x-MnO_x catalysts: (●) 1/30, (▲) 1/45, (■) 1/60, and (◆) 1/120; (a) CO conversion and (b) PROX selectivity.

4.2.2 Effect of Support Molar Ratio

Many Researchers verified that Fe was used to promote the Pt catalysts; therefore the effect of adding Fe_2O_3 to MnO_x support on the PROX activity was studied.

The influence of Fe/Mn molar ratio of $\text{Au/FeO}_x\text{-MnO}_x$ catalyst calcined at 400°C on the catalytic activity in H_2 -rich gas as a function of reaction temperature had two trends, as illustrated in Figure 4.14. The CO conversion and PROX selectivity of Fe:Mn molar ratio of 1:10 and 1:5 molar ratios which have high manganese content increased significantly with reaction temperature from 60 to 160°C as similar as the trend of Au/MnO_x . Unlike Au/FeO_x , the second trend corresponding with Fe:Mn molar ratios of 10:1, 5:1, and 1:1 exhibited high activity at the low temperature. Interestingly, superior activity and selectivity belonged to a Fe:Mn molar ratio of 1:1 with 100% CO conversion, and 56% PROX selectivity at 60°C .

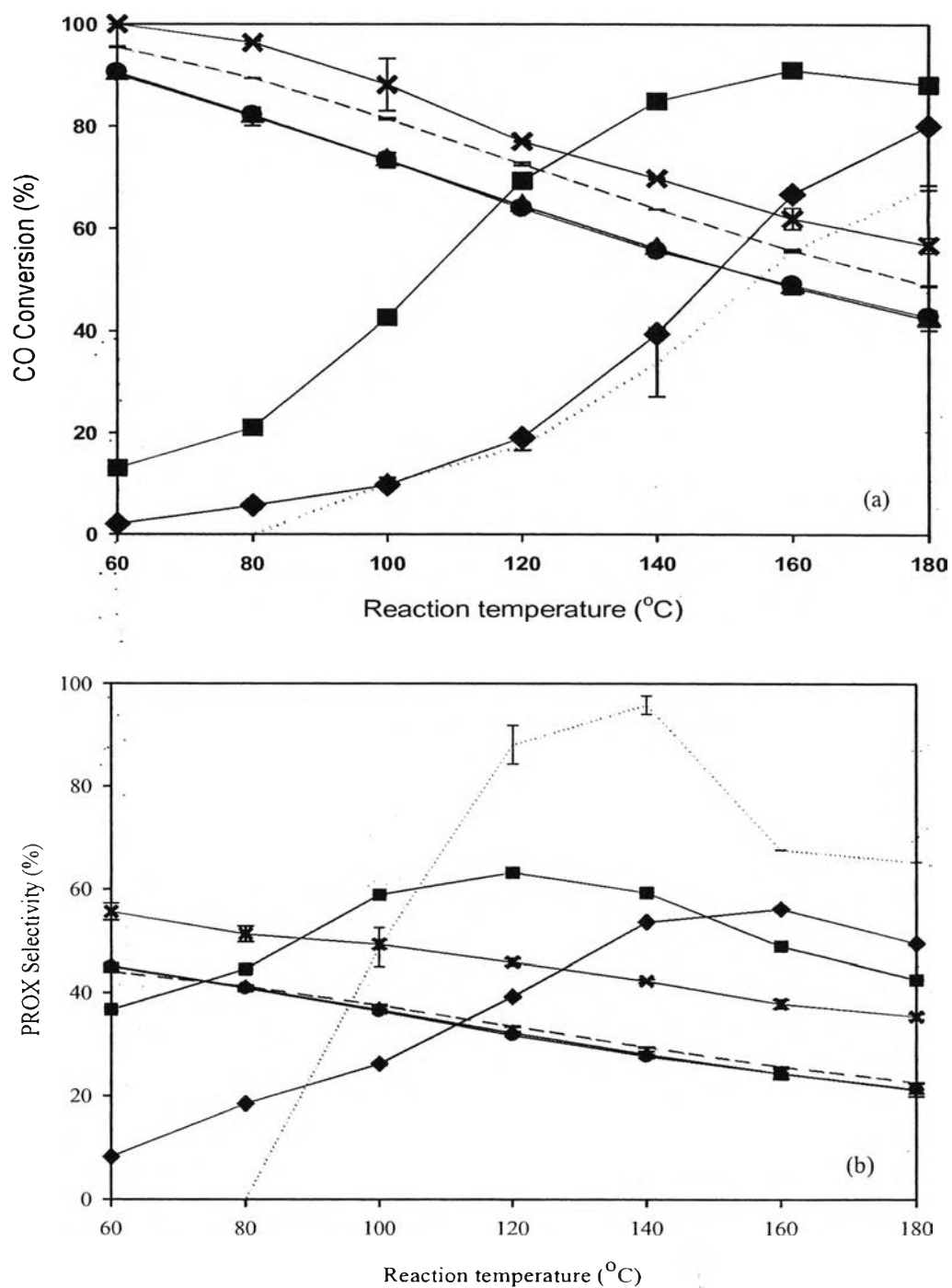
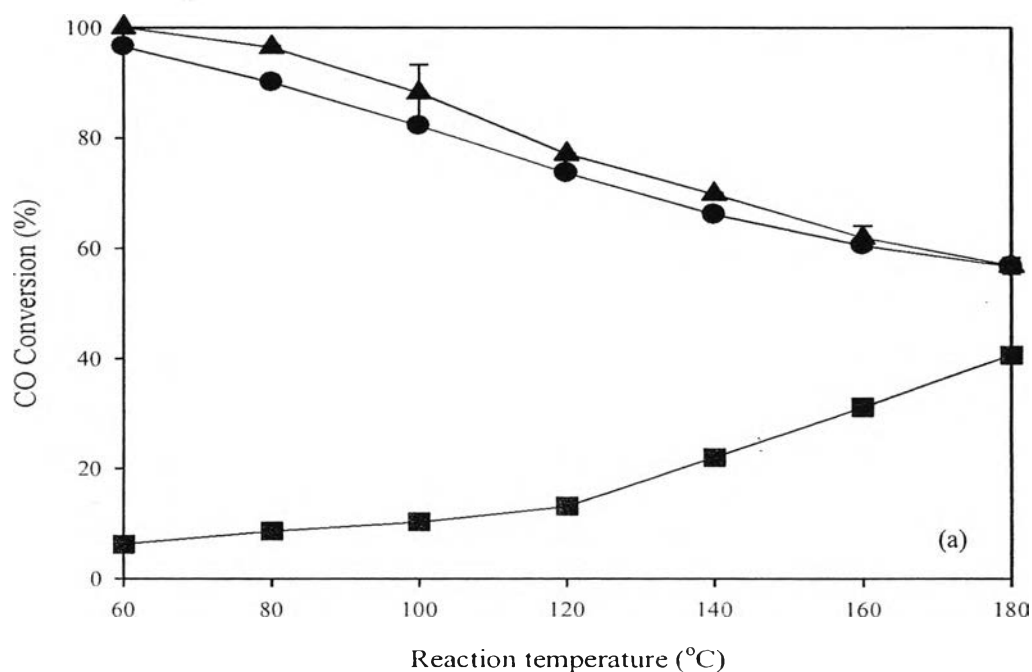


Figure 4.14 Effect of support molar ratio FeO_x-MnO_x on the performance of Au/FeO_x-MnO_x catalysts: (---) FeO_x, (●) 10:1, (▲) 5:1, (x) 1:1, (■) 1:5, (◆) 1:10, and (···) MnO_x; (a) CO conversion and (b) PROX selectivity.

4.2.3 Effect of Calcination Temperature

In this work, the calcination temperature of 400°C was used with this support. Figure 4.15 performs the catalytic behaviors of Au/FeO_x-MnO_x catalysts on various calcination temperatures (300, 400, and 500°C) with atomic ratio of 1/30, and support molar ratio of 1:1. The differences in calcination temperature can be obviously observed that the catalyst calcined at 500°C had distinct activity from others due to different trend of CO conversion—widely increased with the whole range of reaction temperature (60–180°C). For catalysis calcined at 300 and 400°C, the catalysis activity decreased with reaction temperature. The catalyst calcined at 400°C presented the highest activity almost 100% CO conversion and 56% CO selectivity at 60°C.

The XRD results shown in figure 4.4 could also occurred for the observed change in CO conversion with calcinations temperature. The Fe₂O₃ phases was observed at 33.15°, 35.65°, and 54.10° for the catalyst calcined at 500°C (pattern a). This suggests that the catalyst calcined at 500°C is less than those calcined at 300 and 400°C due to sintering of metallic gold particles. In addition, the presence of Fe₂O₃ could cause the difference in the catalytic activity.



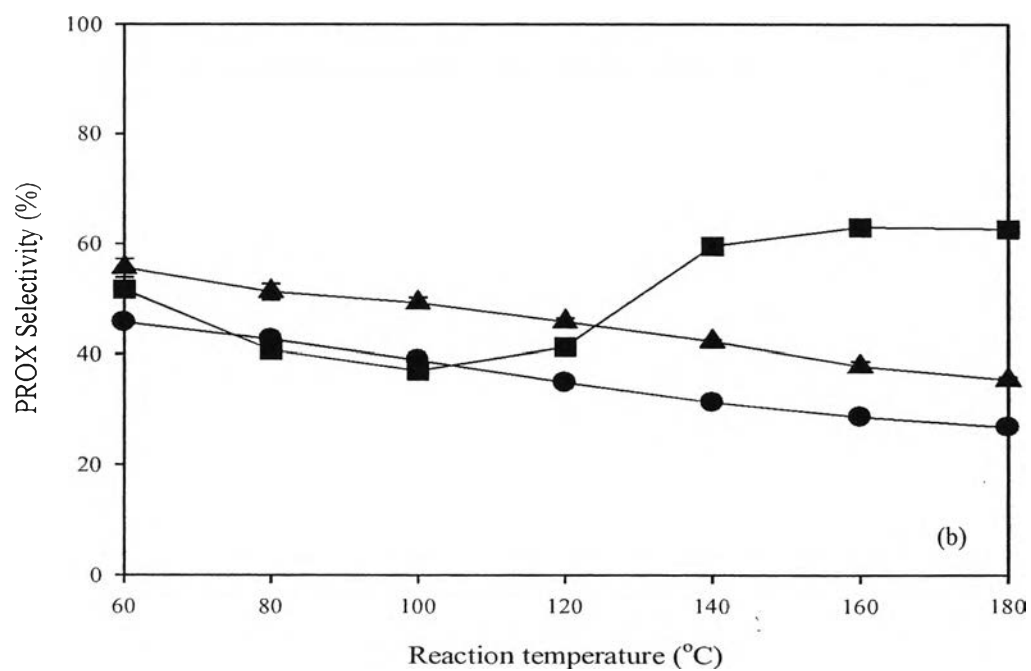
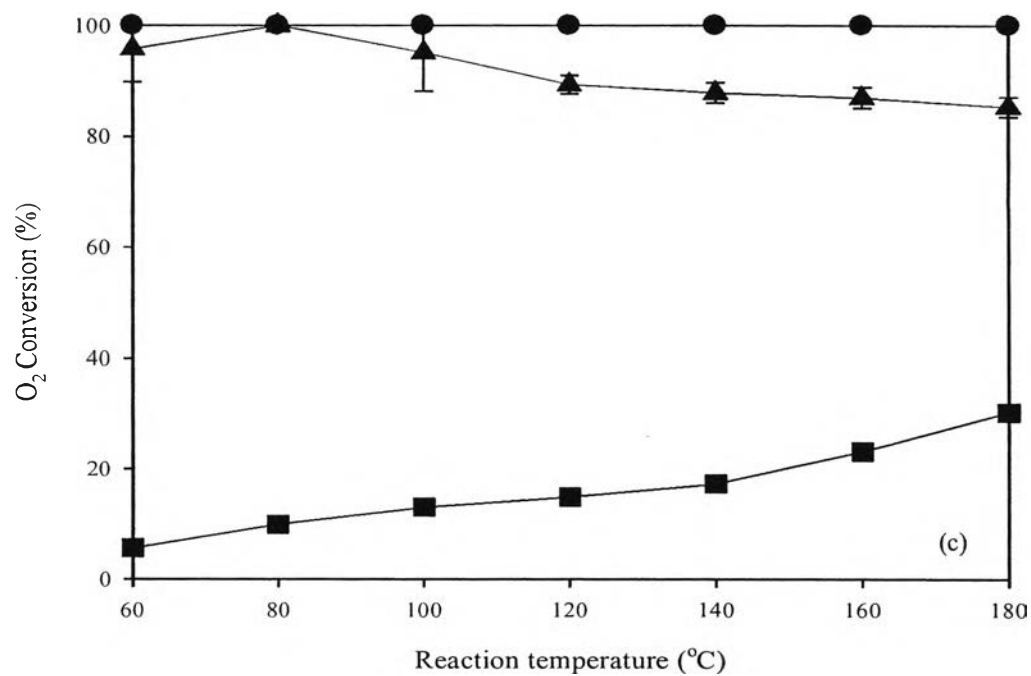


Figure 4.15 Effect of calcination temperature on Au/FeO_x-MnO_x catalyst: (●) 300°C, (▲) 400°C, and (■) 500°C; (a) CO conversion, (b) O₂ conversion, and (c) PROX selectivity.

4.2.4 Effect of Catalyst Pretreatment

It has been reported that pretreatment gas condition can affect on the structure and activity of the supported gold catalysts. In the present study, there are 2 pretreatment conditions which the catalysts were pretreated by He, and O₂ prior to reaction. The comparison between PROX activities of different pretreatment conditions of Au/FeO_x-MnO_x calcined at 400°C with atomic ratio of 1/30, and support molar ratio of 1:1 versus temperature is shown in Figure 4.16. It is clear that the Au/FeO_x-MnO_x pretreated by O₂ was an active catalyst compared to the catalyst pretreated with He. It is therefore of interest to investigate surface changes under different pretreatments. From XRD results, it appears that the size of Au particle was not affected much by pretreatments. However, the formation of Fe₂O₃ as the hematite phase may play an important role in the catalytic performance (Tanielyan *et al.*, 1992 and Kahlich *et al.*, 1997). To better understand the formation of hematite phase, many literature reviews proposed that O₂ may cause the formation of active support phase corresponding to the high activity in PROX reaction due to the characteristic in O₂ storage. According to this explanation, the O₂ pretreatment was used for further investigating the deactivation test of the prepared catalysts in PROX reaction.

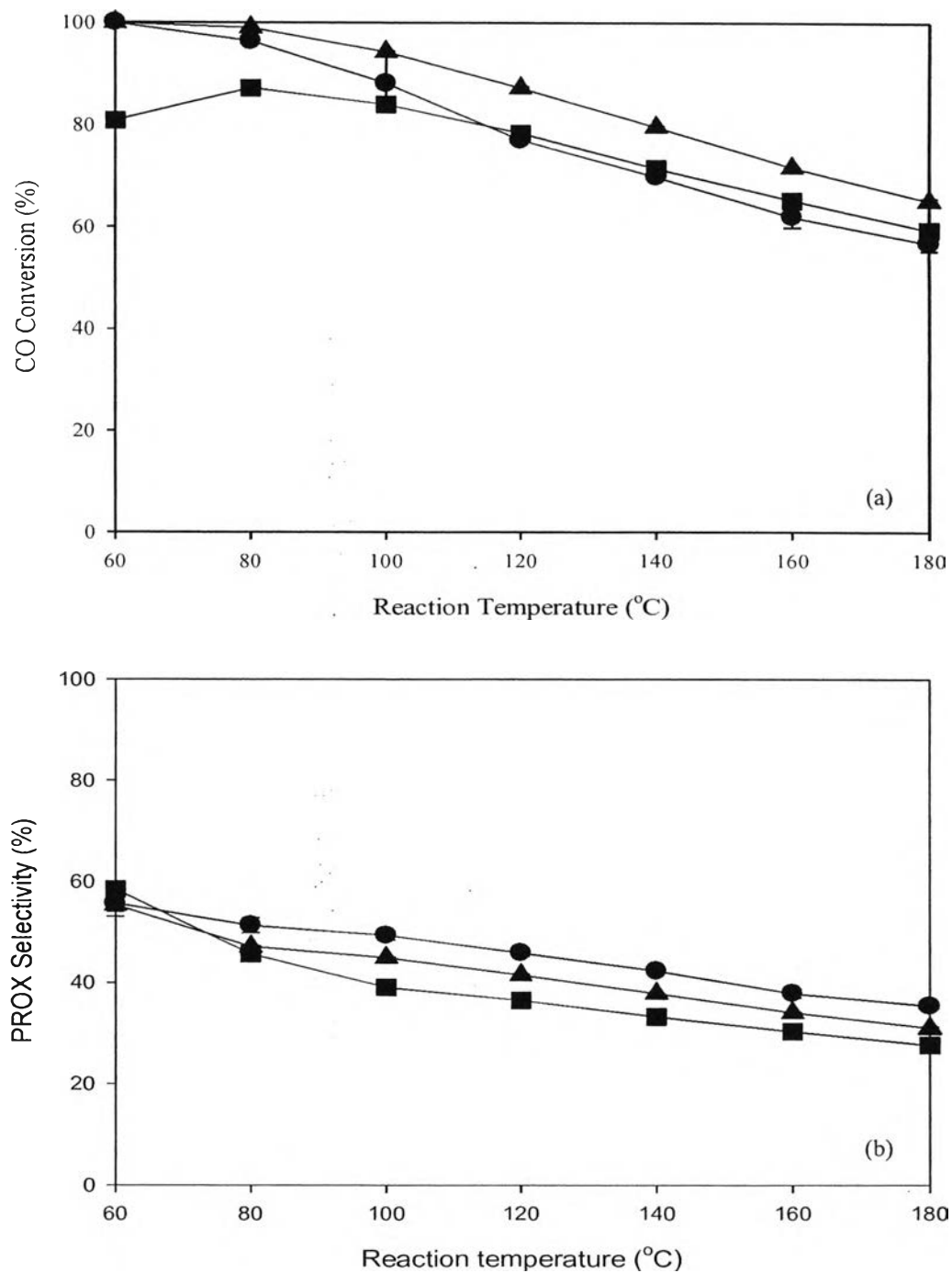


Figure 4.16 Effect of catalyst pretreatment on Au/FeO_x-MnO_x: (●) non-pretreatment, (▲) O₂ pretreatment, and (■) He pretreatment; (a) CO conversion and (b) PROX selectivity.

4.2.5 Deactivation Test

The PROX activity was studied at constant temperature (60°C) for 19 hours in order to observe the stability of the prepared catalysts in the feed consisted of with 1% CO, 1% O₂, and 40% H₂ balanced in He (simulate reformed gas or feed stream) under atmospheric pressure. Ordinarily, the build-up of carbonate species was a key basis of the deactivation of gold based catalysts during PROX of CO reaction as a result of blocking the Au-metal oxide interface (Markus *et al.*, 2004).

Figure 4.17 represents the stability of Au/FeO_x-MnO_x catalyst calcined at 400°C with atomic ratio of 1/30, support molar ratio of 1:1 and pretreated by O₂. It is clearly seen steady activity within 12 h from early stage was found and the small deactivation of Au catalysts was observed. The deactivation is partly caused by the carbonate formation.

4.2.5.1 Effect of H₂O Concentration in the Feed Gas

Normally, the presence of water in the feedstream typically suppressed the catalyst activity, suggesting that blocking active site of catalyst might occur. In the opposite way, the optimum concentration of water improved CO oxidation reaction by transformation of carbonates into thermally less stable bicarbonate species (Daté *et al.*, 2002 and Markus *et al.*, 2004). Fortunately, this catalyst did not only resist H₂O concentration up to 10% but also improve CO conversion (Figure 4.17).

4.2.5.2 Effect of CO₂ Concentration in the Feed Gas

In this work, The aggression negative effect of the presence of CO₂ on the catalytic activity of Au catalyst was more pronounced (Figure 4.17) owing to the formation of carbonates species on the catalyst surface which prevented O₂ adsorption and splitting on support (Srinivas *et al.*, 1996). Therefore, the CO conversion showed in different from with and without water.

4.2.5.3 Effect of Combination of CO₂ and H₂O on Feed Gas

Avgouropoulos *et al.*, 2002 investigated the influence of CO₂ and H₂O on the PROX activities over a Au/ α -Fe₂O₃ catalyst. They reported that the presence of CO₂ and H₂O in feedstream reduced the CO conversion, but increased the CO selectivity. Similar to the previous work, the effect of combination of CO₂ and H₂O presented in the feedstream on the catalytic performance of the prepared

catalysts also indicated the negative effect on catalytic behavior of Au/FeO_x-MnO_x catalyst as shown in Figure 4.17.

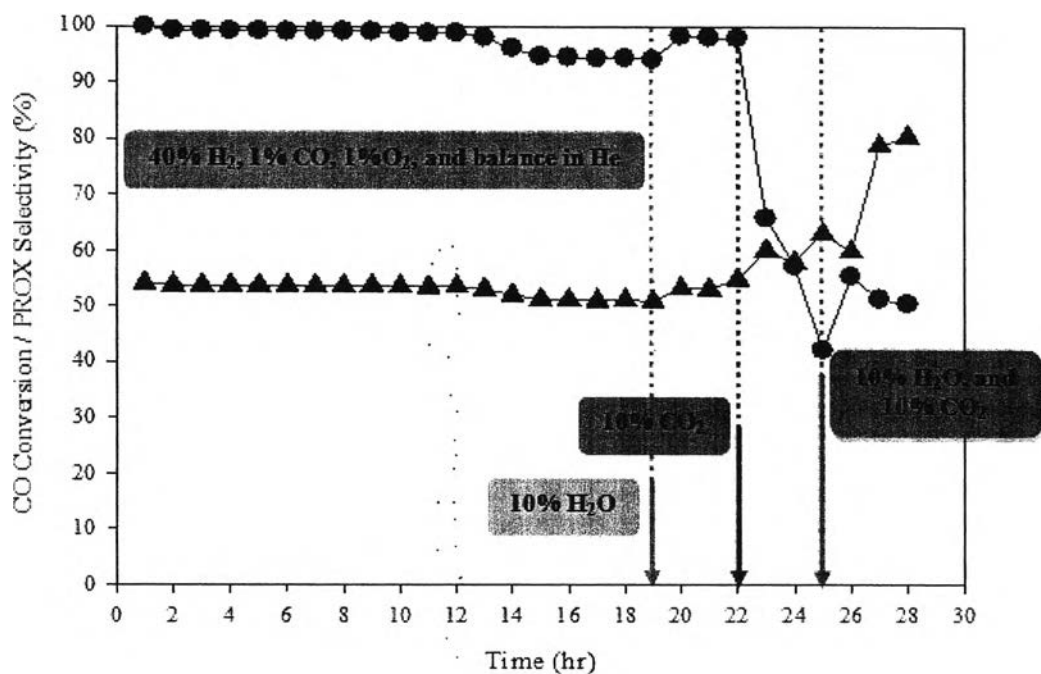


Figure 4.17 Deactivation test of Au/FeO_x-MnO_x catalyst: (●) CO conversion and (▲) PROX selectivity.

4.2.6 Fuel Processing System

After the optimum condition was found in PROX reaction, and a Methanol Fuel Processor (MFP) was then studied. From previous study (Naknam *et al.*, 2009), the optimum catalyst condition for development in an MFP was found at a methanol/water molar ratio of 1 to 1.3 with a total flow rate of 3 ml/min under He carrier gas of 34 ml/min, and catalyst weight (shift max 240) of 1g at a reaction temperature of 250°C.

Based on above description, the catalytic activity was investigated and compare the effect on realistic reformat gas on the activity of Au/FeO_x-MnO_x. Figure 4.18 represents the activity of Au/FeO_x-MnO_x catalyst calcined at 400°C with a Au/FeO_x-MnO_x atomic ratio of 1/30, and a Fe:Mn molar ratio of 1:1, pretreated with O₂ at 60°C for 12 hours. In these operating conditions, it exhibited also a stable catalytic performance and high CO conversion up to 80% during the tested time.

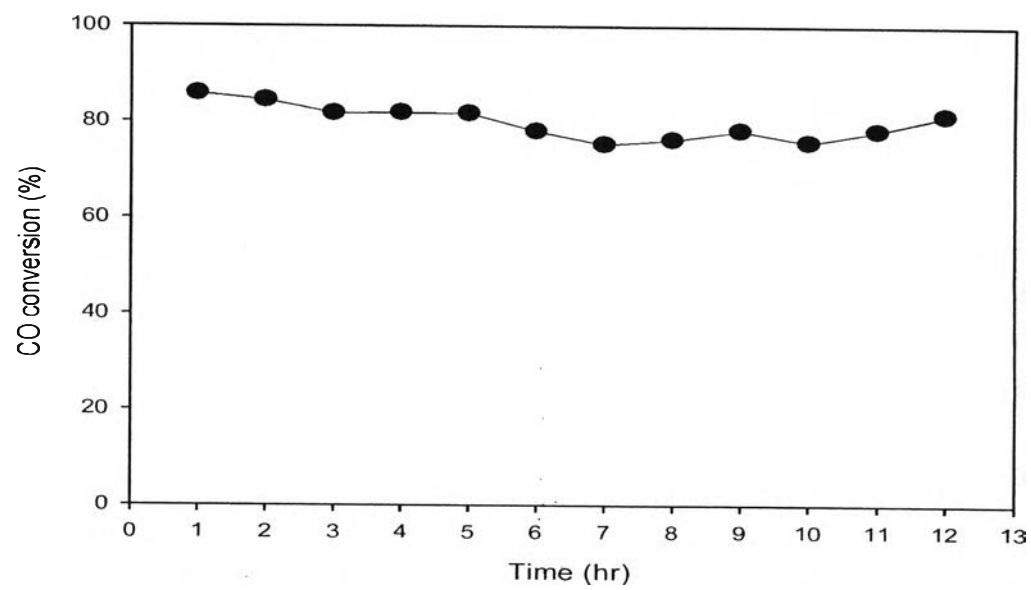


Figure 4.18 Stability test of Au/FeO_x-MnO_x catalyst in methanol fuel processor: (●) CO conversion.